High-speed Avalanche Photodiodes toward 100-Gbit/s per Lambda Era

Masahiro Nada, Toshihide Yoshimatsu, Fumito Nakajima, Hideaki Matsuzaki, and Kimikazu Sano

Abstract

We have developed an avalanche photodiode (APD) in an effort to achieve 100-Gbit/s operation with a single wavelength (100-Gbit/s/lambda). The APD features a gap-grading layer and was set between the absorber and avalanche layers. It achieved an operating bandwidth of 42 GHz in low-gain conditions. An optical receiver made with the APD demonstrated 106-Gbit/s 4-level pulse amplitude modulation operation and 40-km optical amplifier-free transmission over a single-mode fiber under assumption of a KP4 forward error correction threshold.

Keywords: avalanche photodiode (APD), 100-Gbit/s PAM4, datacenter, optical receiver

1. Introduction

The interest in optical fiber communications systems in the last few decades has primarily been focused on long-haul systems capable of handling transcontinental communications and country-to-country communications. Such long-haul systems have included advanced optical devices used for optical communications as well as advanced modulation formats and detection mechanisms. One important example is digital coherent systems [1]. Coherent detection techniques used in combination with digital signal processors have achieved transmission distances of several thousand kilometers, and the development of densely integrated optical transmitters and receivers has enabled digital coherent systems to reach a transmission capacity of over 100 Gbit/s.

Recent interest in optical fiber communications systems has been focused on short-reach applications as represented by inter/intra-datacenter networking. In 2010, 100-Gbit/s Ethernet, which utilizes a bit rate per wavelength of 25 Gbit/s, was standardized for such purposes [2], and the required bit rate per wavelength is now approaching 100 Gbit/s (100-Gbit/s/lambda). Unlike digital coherent systems, such short-reach networks are required to be low-cost and thus simple in structure. Consequently, the network systems and optical components used in short-reach networks must achieve larger capacity and longer transmission distances by using simple direct detection mechanisms and high-speed optical components.

An avalanche photodiode (APD) is a key device to meet such requirements. Avalanche multiplication is initiated by electrons and holes in the APD, which provides a built-in first stage of gain of the electrical signals. Therefore, APDs obtain higher responsivity compared with the conventional PIN-PDs (positive-intrinsic-negative photodiodes), leading to higher sensitivity of the optical receivers. Thus, they effectively extend the transmission distance. To date, we have demonstrated 25-Gbit/s operation for NRZ (non-return-to zero) signals and 50-Gbit/s operation for 4-level pulse amplitude modulation (PAM4) signals by using the high-speed APDs we developed [3–5].

These high-speed APDs surpass the results of our previous examples and are aimed at achieving 100-Gbit/s/lambda operations. A gap-grading layer introduced between the absorber and the avalanche layers helped to boost the operation speed of the

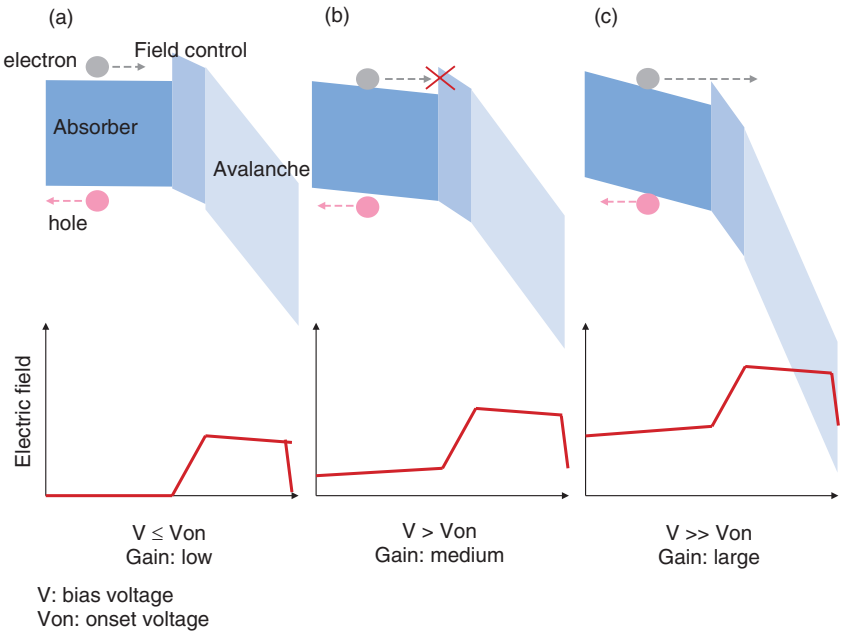

Fig. 1. Schematics of band diagrams of APD for various bias conditions.

APD. An optical receiver fabricated with the APD achieved 106-Gbit/s PAM4 transmission over a 40-km single-mode fiber without using an optical amplifier.

2. Device design and performance

Low-gain operation must be considered when trying to boost the speed of APDs. In principle, there is a strict trade-off between the gain and the speed of the APD according to the gain-bandwidth product (GBP) rule that is governed by the material and thickness of the avalanche layer; that is, the operation speed decreases as the gain increases. Thus, one simple way to obtain high-speed operation is to operate the APD with lower gain. We employ a 90-nm-thick indium aluminium arsenide (InAlAs) avalanche layer, which provides larger GBP as well as low excess noise, in our APD. However, one problem is that a large conduction band offset exists between the indium gallium arsenide (InGaAs) absorber and the InAlAs avalanche layer. This conduction band offset is as large as 0.5 eV, which can be problematic for low-gain and high-speed operation. A schematic band diagram illustrating this issue is shown in **Fig. 1**.

In Fig. 1(a), we show the band diagram around the absorber and the avalanche layer when the bias voltage (V) is lower than the onset voltage (Von). In this condition, the electric field in the absorber is zero, and the potential barrier caused by the conduction band offset remains. The photo-generated electrons and holes do not have drift components; thus, high-speed operation of the APD is not observed in this condition. Additional bias voltage depletes the p-type field control layer, and the electric field in the undoped absorber is invoked, as shown in Fig. 1(b). The photo-generated electrons and holes have drift components in the absorber. However, the remaining potential barrier originating from the conduction band offset prevents electrons from moving toward the avalanche layer. Consequently, high-speed operation cannot be obtained even under the V > Von condition depicted in Fig. 1(b).

To eliminate the potential barrier caused by the conduction band offset, further additional bias voltage is needed (Fig. 1(c)). The additional bias voltage effectively eliminates the potential barrier but simultaneously strengthens the electric field in the avalanche layer, resulting in the increased gain of the APD. Consequently, the speed of the APD is lowered by the GBP limitation.

A gap-grading layer is known to effectively relax the potential barrier [6]. We introduced a 40-nm-thick 1.1-eV indium aluminium gallium arsenide (InAlGaAs) gap-grading layer between the InGaAs absorber and InAlAs avalanche layers to relax the

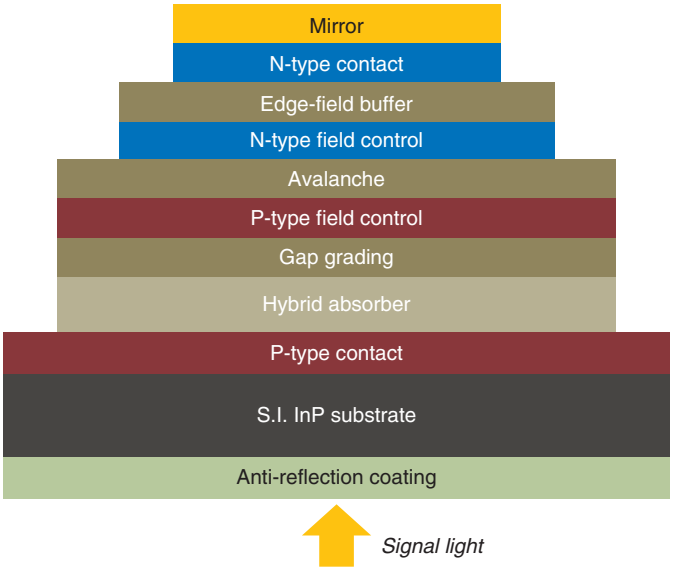

S.I.: semi-insulating
InP: indium phosphide

Fig. 2. Schematic cross-sectional view of the fabricated APD.

potential barrier that prevents the electron transport from the absorber to the avalanche layer under lower bias conditions, which can boost the speed of the APD.

A cross-sectional view of the APD we developed for 100-Gbit/s/lambda (100-Gbit/s PAM4) operation is shown in **Fig. 2**. The APD is designed based on an inverted p-down structure [7]. The epitaxial layers, including the p-type contact, p-type absorber, undoped absorber, gap-grading, p-type field control, avalanche, n-type field control, edge-field buffer, and n-type contact layers are grown on a semi-insulating InP (indium phosphide) substrate by metal-organic chemical vapor deposition. After the epitaxial growth, we formed the triple-mesa structure shown in Fig. 2 using a wet-etching technique. Then we formed the electrodes and mirror metal by electron beam evaporation. The anti-reflection film is coated after the front-end process. Thus, the APD has a back-side illumination structure.

As described above, we employed a 90-nm-thick InAlAs avalanche layer. We also used a hybrid absorber consisting of 150-nm p-type and 150-nm undoped InGaAs to reduce the transit time of the electrons and holes [8].

The current-voltage (I-V) characteristics of the fabricated APD with an active diameter of 14 μm are shown in **Fig. 3**. The photocurrent rapidly rises from 5.5 V to 7.5 V and then increases gradually toward a breakdown voltage (Vb) of 25.4 V due to the avalanche gain. The dark current does not show any unexpected increase, indicating that the APD has no edge breakdown or other unexpected breakdown. The estimated responsivity at unit gain is 0.5 A/W against 1300-nm-wavelength optical input.

The frequency characteristics of the fabricated APD are shown in **Fig. 4**. A maximum bandwidth of 42 GHz was observed with a gain as low as 1.5 thanks to the gap-grading layer in the APD. A bandwidth of over 30 GHz, which is sufficient for 100-Gbit/s PAM4 operation, was maintained for the increase in gain to 3.

3. Receiver characteristics

To demonstrate the 100-Gbit/s PAM4 operation of the APD, we mounted the fabricated APD into a butterfly package together with a transimpedance amplifier and conducted a transmission test with the fabricated APD receiver. The transimpedance amplifier had a bandwidth of 33 GHz, which is sufficient for 100-Gbit/s PAM4 operation. The package has a GPPO electrical output. The optical transmitter we used consisted of a 1309.49-nm-wavelength electro-absorption modulator integrated DFB (distributed feedback) laser (EML) with a launch power of +3.5

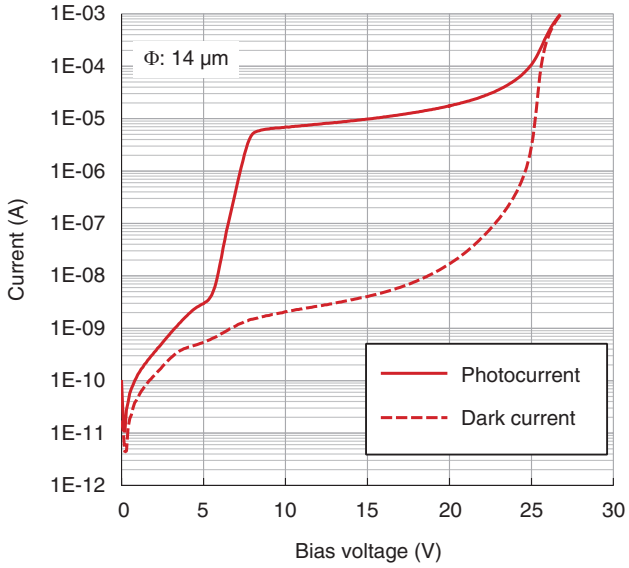

Fig. 3. I-V characteristics of the fabricated APD with an active diameter of 14 μm.

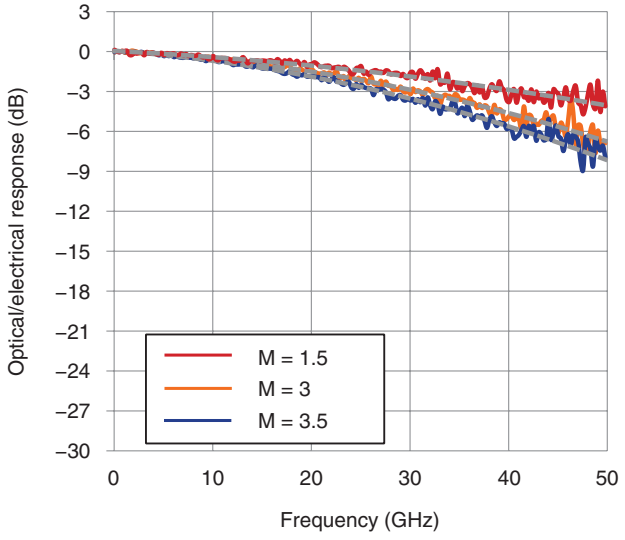

Fig. 4. Frequency characteristics of the fabricated APD.

dBm [9]. The bit rate of the electrical signal that drives the EML was set to be 106-Gbit/s PAM4 by considering the overhead of the forward error correction (FEC). The 106-Gbit/s PAM4, PRBS (pseudo-random binary sequence) signal of 2^{15}-1 was generated with a 3-bit DAC (digital-to-analog converter). The optical output signal from the EML had an extinction ratio at 106-Gbit/s PAM4 operation of about 7 dB. The electrical output signal was captured by a real-time DSO (digital storage oscilloscope) with a 160-GS/s sampling rate and 62-GHz bandwidth.

The transmission tests were performed with offline processing using feed-forward equalization (FFE) with a half-symbol-spaced (T/2-spaced) adaptive equalizer. No pre-emphasis on the transmitter was used. The received power was determined by the VOA (variable optical attenuator) set in front of the receiver. For the 40-km transmission test, we used single-mode fiber (SMF) with a loss of 0.33 dB/km. The measurement setup for the characterization of the APD optical receiver is shown in **Fig. 5**.

The bit error rate (BER) characteristics of the fabricated APD receiver under back-to-back conditions and after 40-km transmission are presented in **Fig. 6(a)**. The number of taps of the FFE was set to be 17 for both conditions. In **Fig. 6(b)** and **(c)**, we respectively show the equalized electrical eye diagrams of the APD receiver for back-to-back and after 40-km transmission conditions. The BER characteristics in Fig. 6(a) indicate that the fabricated APD receiver successfully demonstrated 106-Gbit/s PAM4 operation even for the 40-km transmission over SMF without an optical amplifier, as well as in the back-to-back condition. The 40-km transmission was achieved with an average received power ($P_{avg.}$) of –11.47 dBm at a KP4-FEC limit. The power penalty against the back-to-back condition was 0.32 dB. The eye diagram obtained after 40-km transmission

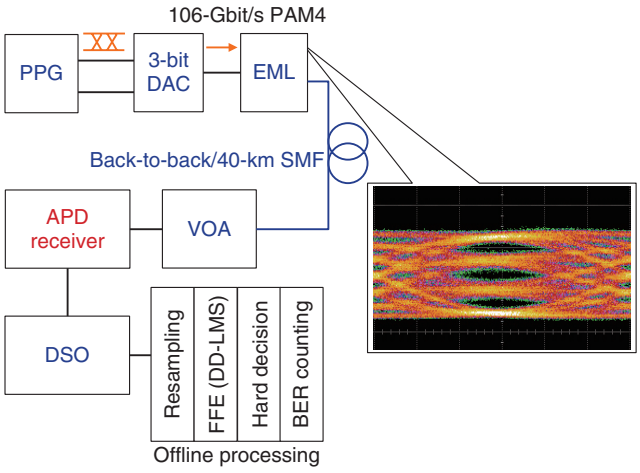

BER: bit error rate
DD-LMS: decision-directed least mean square
PPG: pulse-pattern generator

Fig. 5. Experimental setup for 100-Gbit/s PAM4 bit error rate test utilizing APD receiver.

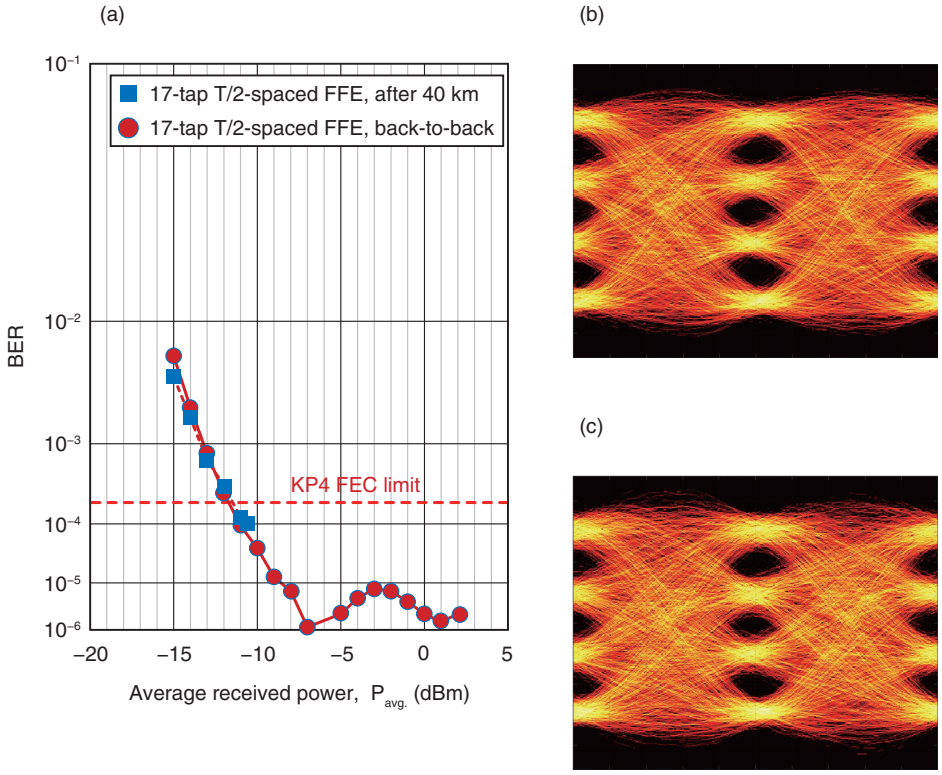

Fig. 6. (a) BER characteristics of the fabricated APD receiver for the back-to-back condition and after 40-km transmission. The T/2-FFE is set to 17 taps. (b) Electrical eye diagram of the APD receiver at back-to-back condition and (c) after 40-km transmission.

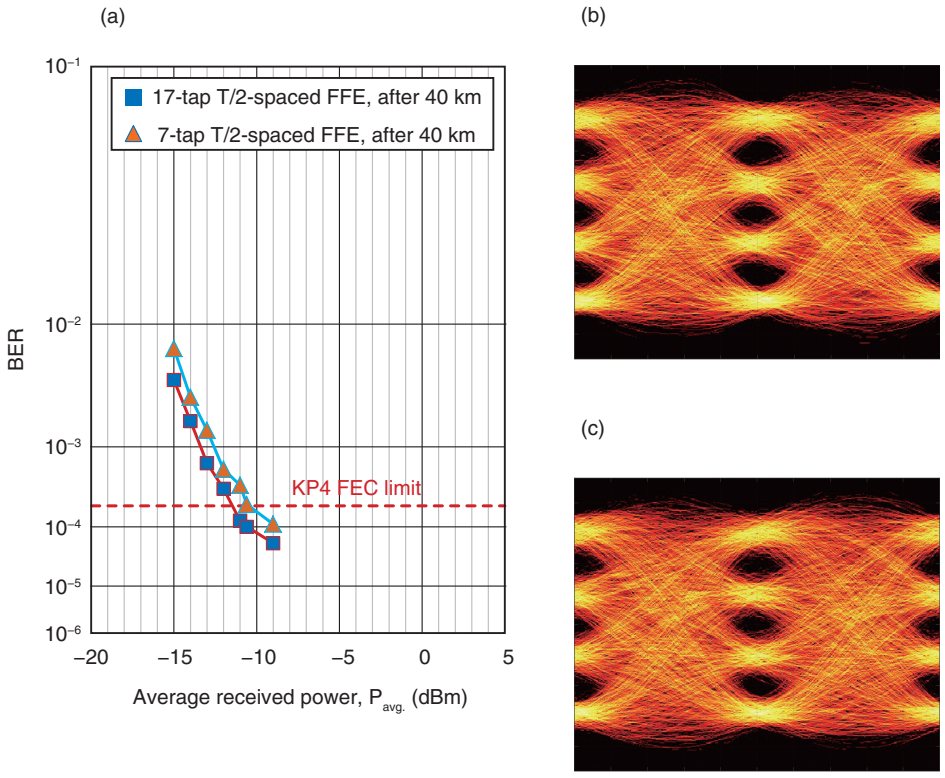

Fig. 7. (a) BER characteristics of the fabricated APD receiver after 40-km transmission for 17-tap and 7-tap conditions, (b) electrical eye diagram of the APD receiver after 40-km transmission with 17 taps, and (c) with 7 taps.

shows no degradation from that of the back-to-back condition.

A smaller number of FFE taps is advantageous in terms of power consumption and latency by signal processing when considering the digital-signal processing used in practical optical transceivers. The BER characteristics of the APD receiver for 17-tap and 7-tap FFE after 40-km transmission are shown in **Fig. 7(a)**. A minimum receiver sensitivity as low as –10.57 dBm was obtained, even with the 7-tap FFE. The equalized eye diagram of the APD receiver with 7-tap FFE is presented in **Fig. 7(b)**. No significant degradation from the 17-tap condition is apparent, which indicates that the 7-tap FFE is also applicable for 40-km transmission without an optical amplifier using the fabricated APD.

4. Conclusion

We developed a high-speed APD designed for use in the 100-Gbit/s per wavelength era. We introduced an optimized gap-grading layer consisting of 1.1-eV InAlGaAs in order to achieve low-gain, high-speed operation. Thanks to the gap-grading layer, the APD exhibited a peak bandwidth of 42 GHz with a responsivity at unit gain of 0.5 A/W. A 30-GHz bandwidth was maintained for a gain of 3. The optical receiver fabricated with the APD successfully achieved 40-km optical-amplifier-free transmission for 106-Gbit/s PAM4 optical signals. These results suggest that the 100-Gbit/s/lambda era can be realized even when extending the transmission distance by using low-power-consumption, cost-effective optical components that high-speed APDs provide.

References

[1] K. Kikuchi, "Digital Coherent Optical Communication Systems: Fundamentals and Future Prospects," IEICE Electronics Express, Vol. 8, No. 20, pp. 1642–1662, 2011.
[2] IEEE P802.3ba 100 Gb/s Ethernet Task Force, http://www.ieee802.org/3/ba/
[3] T. Yoshimatsu, M. Nada, M. Oguma, H. Yokoyama, T. Ohno, Y. Doi, I. Ogawa, and E. Yoshida, "Compact and High-sensitivity 100-Gb/s (4 × 25 Gb/s) APD-ROSA with a LAN-WDM PLC Demultiplexer," Proc. of the 38th European Conference on Optical Communication (ECOC 2012), Th.3.B.5, Amsterdam, The Netherlands, Sept. 2012.
[4] F. Nakajima, M. Nada, and T. Yoshimastu, "High-speed Avalanche Photodiode and High-sensitivity Receiver Optical Subassembly for

100-Gb/s Ethernet," J. Lightw. Technol., Vol. 34, No. 2, pp. 243–248, 2016.
[5] Y. Nakanishi, T. Ohno, T. Yoshimatsu, Y. Doi, F. Nakajima, Y. Muramoto, and H. Sanjoh, "4 x 28 Gbaud PAM4 Integrated ROSA with High-sensitivity APD," Proc. of the 20th Opto-Electronics and Communications Conference (OECC 2015), post-deadline paper, Shanghai, China, June/July 2015.
[6] J. C. Campbell, "Recent Advances in Telecommunications Avalanche Photodiodes," J. Lightw. Technol., Vol. 25, No. 1, pp. 109–121, Jan. 2007.
[7] M. Nada, Y. Muramoto, H. Yokoyama, T. Ishibashi, and H. Matsuzaki, "Triple-mesa Avalanche Photodiode with Inverted P-Down Structure for Reliability and Stability," J. Lightw. Technol., Vol. 32, No. 8, pp. 1543–1548, Apr. 2014.
[8] M. Nada, T. Yoshimatsu, Y. Muramoto, H. Yokoyama, and H. Matsuzaki, "Design and Performance of High-speed Avalanche Photodiodes for 100-Gb/s Systems and Beyond," J. Lightw. Technol., Vol. 33, No. 5, pp. 984–990, 2015.
[9] S. Kanazawa, S. Tsunashima, Y. Nakanishi, Y. Muramoto, H. Yamazaki, Y. Ueda, W. Kobayashi, H. Ishii, and H. Sanjoh, "Equalizer-free 2-km SMF Transmission of 106-Gbit/s 4-PAM Signal Using Optical Transmitter/Receiver with 50 GHz Bandwidth," Proc. of the 21st Opto-Electronics and Communications Conference (OECC 2016), ThD1-2, Niigata, Japan, July 2016.

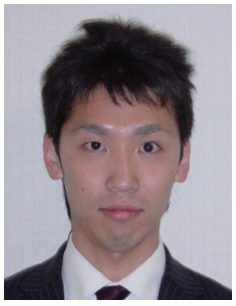

Masahiro Nada
Research Engineer, NTT Device Innovation Center.
He received an M.E. in applied physics from the University of Electro-Communications, Tokyo, in 2009 and a Ph.D. in engineering from the University of Tokyo in 2017. He joined NTT Photonics Laboratories in 2009 and has since been researching and developing high-speed, high-responsivity APDs and their applications in optical fiber communications systems. Dr. Nada received the Young Researcher's Award from the Institute of Electronics, Information and Communication Engineers (IEICE) in 2014. He is a member of IEICE, the Optical Society (OSA), and the Institute of Electrical and Electronics Engineers (IEEE).

Toshihide Yoshimatsu
Senior Research Engineer, NTT Device Innovation Center.
He received a B.E. and M.E. in applied physics from Tohoku University, Miyagi, in 1998 and 2000. He joined NTT Photonics Laboratories in 2000. He is involved in researching and developing ultrafast opto-electronic devices. He received the International Conference on Solid State Devices and Materials (SSDM) Paper Award in 2004. He is a member of IEICE and the Japan Society of Applied Physics (JSAP).

Fumito Nakajima
Senior Research Engineer, NTT Device Technology Laboratories.
He received a B.E., M.E., and Ph.D. from Hokkaido University in 1998, 2000, and 2003. He joined NTT Photonics Laboratories in 2003. He is involved in the research and development (R&D) of high-speed photodiodes and APDs for optical receivers. He received the Young Researcher's Award in 2006 and the Achievement Award in 2018 from IEICE. Dr. Nakajima is a member of IEICE.

Hideaki Matsuzaki
Senior Research Engineer, Supervisor, NTT Device Technology Laboratories.
He received a B.S. and M.S. in physics from Kyoto University in 1993 and 1995. He joined NTT's Atsugi Electrical Communications Laboratories in 1995. He is currently engaged in R&D of compound semiconductor devices, photodiodes, and laser diodes. He is a member of IEICE.

Kimikazu Sano
Senior Research Engineer, Supervisor, NTT Device Innovation Center.
He received a B.S., M.S., and Ph.D. in electrical engineering from Waseda University, Tokyo, in 1994, 1996, and 2004. He joined NTT in 1996. Since then, he has been designing and evaluating ultrafast integrated circuits (ICs) and optoelectronic ICs. From 2005 to 2006, he was a visiting researcher at the University of California, Los Angeles (UCLA), USA, where he researched a microwave/millimeter-wave sensing system. He was with NTT Electronics from 2012 to 2014, where he developed high-speed analog ICs and packaged modules for coherent optical systems. He is currently developing lasers, photodiodes, and analog ICs for optical metro-access networks. He served as a member of the Technical Program Committee for the IEEE Compound Semiconductor IC Symposium (CSICS) from 2008 to 2010.